

# MINERALOGICAL MAGAZINE

VOLUME 37 NUMBER 289 MARCH 1970

---

## Phase relations in some tholeiitic lavas illustrated by the system $R_2O_3-XO-YO-ZO_2$

BRIAN G. JAMIESON, Ph.D.

Grant Institute of Geology, University of Edinburgh

**SUMMARY.** In order to aid the graphical presentation of analyses of igneous rocks, a pseudo-quaternary system  $R_2O_3-XO-YO-ZO_2$  has recently been used (O'Hara, 1968, fig. 4). To test its ability to present the analytical data of tholeiitic basalts, the analyses of selected lavas have been projected into the system and then sub-projected into two planes. Lines, which represent the loci of liquid compositions in certain isobaric, pseudo-univariant equilibria, have been drawn on the basis of the melting relations of the basalts. After reading the pseudo-ternary phase diagrams resulting from the sub-projections, some genetic aspects of the lavas of Kilauea and Mauna Loa are discussed from a phase equilibrium standpoint.

CHEMICAL, mineralogical, and textural features of basic igneous rocks have been extensively described with reference to phase relations in synthetic systems such as  $CaMgSi_2O_6-Mg_2SiO_4-CaAl_2Si_2O_8-SiO_2$  and the bounding ternary faces (e.g. Bowen, 1914, 1928; Osborn and Tait, 1952). In general there is a similarity between phase assemblages and crystallization behaviour in the synthetic and natural systems. However, since only 4 of the 12 major and minor oxides in basic rocks are included in the synthetic system, the similarity between the crystallization of synthetic melts and basaltic magma should not be overstressed.

During the past decade experimental studies on natural basalts have led towards an understanding of crystallization behaviour in the complex basaltic system. Atmospheric-pressure quenching experiments have defined the melting histories of some 50 tholeiitic basalts (Yoder and Tilley, 1962; Tilley *et al.*, 1963, 1964, 1965, 1966; Cohen *et al.*, 1967). From the results of these investigations it is possible to estimate the essential features of phase relations in the natural basaltic system with its 12 major and minor components. The graphical presentation of phase relations in a 12 component system does, however, present considerable geometrical problems.

With this difficulty in mind, O'Hara (1968, fig. 4), by considering chemical affinities between cations in basic magmas, has used a scheme that allows 10 of the major and minor oxides of basic rocks to be expressed in terms of 4 components. To avoid confusion with the analogous synthetic system,  $Al_2O_3-CaO-MgO-SiO_2$ , these components

are labelled  $R_2O_3$ -XO-YO-ZO<sub>2</sub> rather than A-C-M-S (O'Hara, 1968, fig. 4). However, apart from this nomenclature change the projection system described below is identical to that used by O'Hara.

Once analyses of basalts have been projected into the system  $R_2O_3$ -XO-YO-ZO<sub>2</sub> it becomes feasible to present, by means of sub-projections, the phase relations recorded in the melting experiments described above.

Using data projection schemes, constructions of partial natural phase diagrams from basalt analyses have been made by Coombs (1963), Muir and Tilley (1964, fig. 6), and O'Hara (1965, figs. 2 and 3). These authors, however, considered normative diopside, plagioclase, olivine, and quartz. The present scheme, involving the projection of a greater part of each analysis into a pseudo-quaternary system before sub-projections are made and phase boundaries constructed, is a refinement of these constructions, and it appears to have the following advantages:

Although coordinates are calculated on a weight percent basis, the calculation, for example, of all FeO, MnO, and MgO as YO avoids the distortion brought about by varying the Fe/Mg ratio in a C.I.P.W. normative plot.

A larger proportion of an analysis is taken into consideration; perhaps the most significant inclusion is K<sub>2</sub>O, which is mineralogically expressed as alkali feldspar, which plots at the plagioclase composition point.

Since almost all the major minerals of basic and ultra-basic rocks plot in the system  $R_2O_3$ -XO-YO-ZO<sub>2</sub>, a large number of projection points and planes are available. As described by O'Hara, a computer program has been written to calculate the coordinates of analyses in the main projection and in the various sub-projections. Up to 12 of these coordinates are printed out and the petrologist need consider only those applicable to his specific problem.

*Procedure.* This paper demonstrates the ability of the  $R_2O_3$ -XO-YO-ZO<sub>2</sub> data projections scheme to reproduce the phase relations during the early crystallization of Hawaiian tholeiitic lavas at low pressure. This has been done by constructing phase diagrams from the analyses and atmospheric-pressure melting histories of basalts for which these data exist. The internal consistency of these diagrams is assessed by inspection. Following this the analyses of various porphyritic lavas of Kilauea and Mauna Loa have been plotted in the diagrams to ascertain the agreement between the constructed phase boundaries, phenocryst assemblages, and postulated genetic relationships.

The exercise has been carried out using analysis of tholeiitic basalts for two reasons: firstly, most available melting data are for tholeiitic basalts and, secondly, because of simpler mineralogy, the fractionation of tholeiitic magma is better understood than that of alkali basalt magma. However, a few other basalts have been used to help delimit the phase boundaries, viz the high-Al<sub>2</sub>O<sub>3</sub> basalt from the Medicine Lake Highlands, W (Yoder and Tilley, 1962, table 2, no. 16), and the alkali basalts, Hu, from Hawaii (Yoder and Tilley, 1962, table 2, no. 20), and E<sub>1</sub>, from Iceland (Tilley *et al.*, 1964, table 1). The latter pair contain, respectively, 2.2 and 0.57 % *ne* in the norm.

Among the various sub-projections available, two seem best suited to display, with a minimum of distortion, the composition points of, and the phase boundaries for, tholeiitic rocks: a projection to, or from, the olivine composition point into the plane  $R_2O_3-XO.ZO_2-YO.ZO_2$ , the olivine projection (O'Hara, 1968, fig. 4); and a projection to, or from, the clinopyroxene composition point into the plane  $YO-ZO_2-XO.R_2O_3$ , the clinopyroxene projection (O'Hara, 1968, fig. 6).

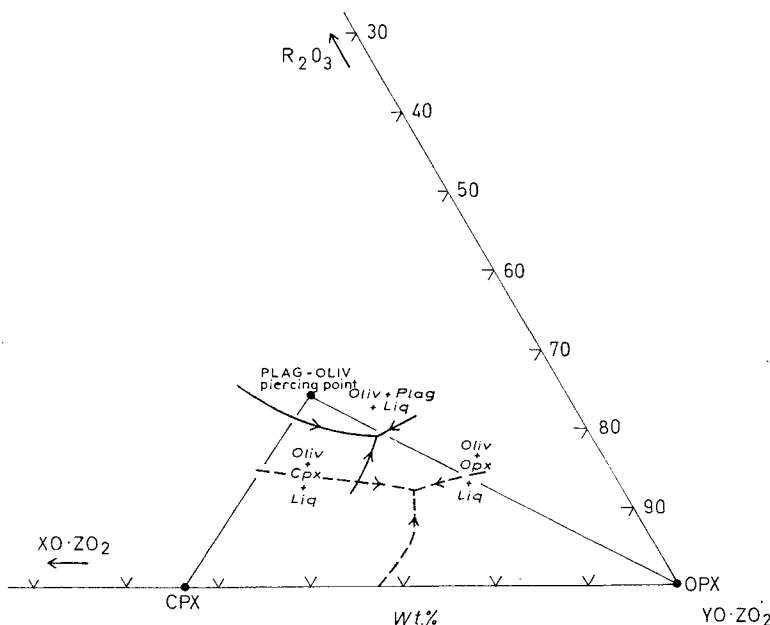


FIG. 1. Part of the plane  $R_2O_3-XO.ZO_2-YO.ZO_2$  in the system  $R_2O_3-XO-YO-ZO_2$ . Mineral compositions and the phase relations on the boundary of the olivine primary phase volume are projected into this plane from the olivine composition point. Isobaric phase boundaries (full lines) have been constructed from basalt melting relations and the appropriate isobaric divariant assemblages are indicated; broken lines represent the analogous isobaric univariant phase boundaries in the synthetic system  $Al_2O_3-CaO-MgO-SiO_2$ .

The distribution of projected basalt composition points enables the phase relations to be constructed on the boundary of the olivine and clinopyroxene primary phase volumes.

Fig. 1 shows the position of the principal basaltic minerals when projected from olivine. Also projected are broken lines, which are the loci of liquid compositions in some of the isobaric univariant equilibria bounding the olivine primary phase volume in the synthetic system  $Al_2O_3-CaO-MgO-SiO_2$ . Full lines, similarly, represent the loci of liquid compositions in isobaric pseudo-univariant equilibria in the pseudo-quaternary system  $R_2O_3-XO-YO-ZO_2$ , which are indicated by the melting relations of Hawaiian basalts.

Fig. 2 shows all the above features, except the phase relations in the synthetic quaternary system, for the clinopyroxene projection. The lavas used are given in an

appendix. Brief petrographic notes and, whenever relevant, the melting relations are also tabulated.

*Olivine projection.* Fig. 3 is a projection from, or towards, olivine of the analyses of basalts for which equilibrium phase relations are known, and which had olivine as liquidus or second phase in the melting experiments. Strictly, the projection should be

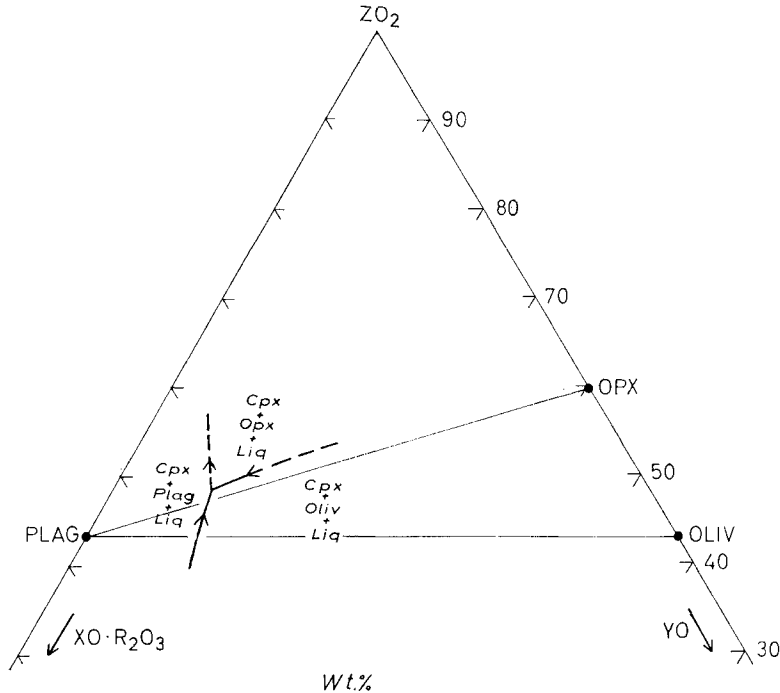


FIG. 2. Part of the plane  $YO-ZO_2-XO.R_2O_3$  in the system  $R_2O_3-XO-YO-ZO_2$ . Mineral compositions and the phase relations on the boundary of the clinopyroxene primary phase volume are projected into this plane from the clinopyroxene composition point. The isobaric univariant phase boundaries have been constructed from basalt melting relations and the appropriate isobaric divariant assemblages are indicated.

used only for basalts with olivine as liquidus phase; those with olivine as second phase are usually dealt with satisfactorily. Distortion is introduced when olivine is the third or later phase to crystallize.

The equilibria bounding the olivine primary phase volume have been constructed by taking account of the melting relations of the basalts, in particular the relative order of disappearance of the phases.

An isobaric, pseudo-invariant equilibrium involving clinopyroxene, olivine, plagioclase, orthopyroxene, and liquid is indicated at the approximate projected position  $R_2O_3$  19%,  $XO.ZO_2$  24%,  $YO.ZO_2$  57%; i.e. the liquid that coexists at equilibrium with these four solid phases at atmospheric pressure has a composition projecting into the plane at this point.



normal ternary. If olivine is the liquidus phase in a magma the projected composition of the liquid does not change its position until the second phase starts to precipitate, i.e. when the liquid composition reaches the boundary of the olivine primary phase volume.

The probable crystallization histories of tholeiitic basalts can be inferred from fig. 3, the whole-rock analyses being assumed to correspond to the composition of the original, almost-all-liquid magma. This is, of course, not a valid assumption in the case of a cumulus-enriched magma.

Magmas with compositions such as the Hawaiian ankaramite from Mauna Kea (MK) and the Kilauean prehistoric basalt (Kp) would first precipitate olivine. With falling temperature clinopyroxene would join olivine as a precipitating phase. At this stage the liquid compositions would, in projection, describe individual paths towards the line representing liquid compositions in the isobaric, pseudo-univariant equilibrium clinopyroxene+plagioclase+olivine+liquid. Once this pseudo-univariant condition is reached, plagioclase would start to precipitate, along with the other two solid phases, while the liquid compositions would move along the boundary curve towards the isobaric, pseudo-invariant, five-phase point. Assuming equilibrium crystallization, magma with a composition similar to MK and Kp would, depending on its initial composition, almost completely freeze either in the pseudo-invariant condition or before it was reached.

Perfect fractional crystallization, in contrast, would produce successive 1, 2, and 3-phase layered accumulates; the course of crystallization would pass through the isobaric, pseudo-invariant condition described above because it is an equilibrium involving resorption. Residual liquid compositions would move towards liquid compositions in the pseudo-eutectic, isobaric, pseudo-invariant equilibrium clinopyroxene+orthopyroxene+plagioclase+silica+liquid. This equilibrium occurs at a temperature lower than the pseudo-invariant equilibrium involving olivine instead of silica.

In a similar manner, magmas close in composition to Hu, NM<sub>5</sub> and E<sub>2</sub>, all of which project in the plagioclase+olivine field of fig. 3, would precipitate olivine, joined by plagioclase, with clinopyroxene as the third solid phase.

Basaltic magmas with compositions projecting in the remaining isobaric, pseudo-divariant area, the orthopyroxene+olivine field, e.g. Ko, Ka, and ML<sub>1887</sub>, would crystallize orthopyroxene as second phase.

*Clinopyroxene projection.* Fig. 4 shows the sub-projection from, and towards, the clinopyroxene composition point of the analyses of melted tholeiites. This projection is a necessary complement of the olivine projection as it shows the position of the composition points relative to the olivine composition point.

Although it is liquidus phase only in the more Fe-rich basalts, clinopyroxene was encountered in the presence of liquid in all the melting experiments. It was frequently the penultimate solid phase to melt entirely. Nevertheless, to avoid any distortion, only those basalts with clinopyroxene as liquidus or second solid phase have been plotted.

In fig. 4 the isobaric, pseudo-invariant liquid composition is at the approximate position YO 10 %, ZO<sub>2</sub> 48 %, XO.R<sub>2</sub>O<sub>3</sub> 42 %.

The location of boundary curves cannot be carried out with the same degree of certainty as in the olivine projection. Considering melting relations alone, only two basalts have compositions that should project on to boundary curves, viz the Kilauea basalt  $K_{1955/77}$  and the Medicine Lake Highlands basalt, W. Both of these lose olivine and plagioclase simultaneously in the melting experiments.

There is little unambiguous evidence bearing on the position of the boundary

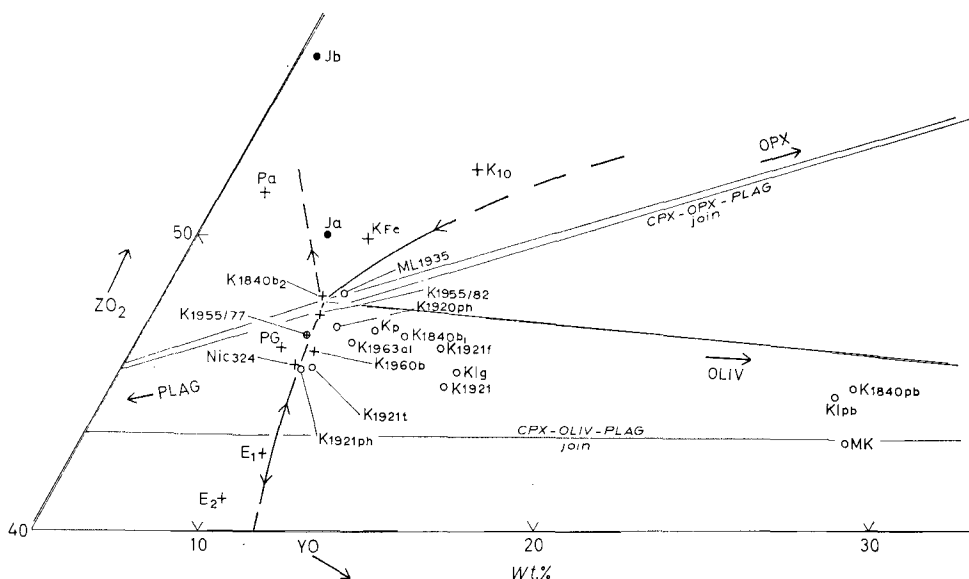


FIG. 4. Part of the plane  $YO-ZO_2-XO.R_2O_3$ . Selected analyses of melted basalts are projected from the clinopyroxene composition point into the plane. The phase boundaries have been constructed on the basis of the melting relations of the lavas. Crosses represent basalts with plagioclase as second solid phase, after clinopyroxene, or, in some cases, as liquidus phase. Similarly circles represent basalts with olivine as second or liquidus phase. The composition points of olivine, orthopyroxene, and plagioclase in the projection plane are shown in fig. 2. The significance of  $J_a$  and  $J_b$  is discussed in the text.

curves between the orthopyroxene+clinopyroxene and plagioclase+clinopyroxene fields and between the olivine+clinopyroxene and orthopyroxene+clinopyroxene fields.

In this clinopyroxene projection are included analyses of olivine-poor lavas with bulk compositions that are indicative of considerable fractionation. It is, therefore, appropriate at this stage to consider the validity of the analogy between natural magmas and the synthetic quaternary  $Al_2O_3-CaO-MgO-SiO_2$  as fractionation proceeds and a diminishing proportion of the bulk analysis is contained within the system  $Al_2O_3-CaO-MgO-SiO_2$ . This analogy, of course, forms the basis of the  $R_2O_3-XO-YO-ZO_2$  projection scheme.

With increasing  $(Na+K)/Ca$  ratio the projection scheme breaks down and should not be used when alkali feldspar starts to precipitate.

As the  $Fe/Mg$  ratio increases and  $FeO$  accounts for an increasingly large

proportion of YO the analogy also breaks down. The solidification of evolved basaltic magmas with high Fe/Mg ratios involves too many variables, and hence has too many degrees of freedom to allow a well-defined pseudo-quaternary diagram to be constructed. A consideration of the two segregation veins  $K_{Fe}$  and  $K_{10}$  (Kuno *et al.*, 1957, table 5, no. 6; Tilley *et al.*, 1963, table 3, no. 7) shows that this stage appears to have been attained with these compositions. The melting history of  $K_{10}$  records clinopyroxene as liquidus phase at 1120 °C with plagioclase following at 1110 °C, while  $K_{Fe}$  shows the simultaneous entry of these two phases at 1080 °C (Tilley *et al.*, 1963, fig. 12).<sup>1</sup> These melting histories imply that the projected composition points should lie close to the boundary, in fig. 4, between the orthopyroxene+clinopyroxene and plagioclase+clinopyroxene fields.

It must be stressed that these segregation veins display an extreme degree of Fe enrichment relative to the parental host basalt (Kuno, 1965, fig. 3). Before accepting the boundary curve indicated by the plotted position of these veins, it is therefore instructive to consider, and to compare with  $K_{10}$  and  $K_{Fe}$ , the plot, in fig. 4, of the analysis of a basaltic segregation vein Jb that shows little Fe enrichment but considerable Si enrichment.

$J_b$  is a segregation vein in  $J_a$ , an 'olivine andesite' or tholeiitic andesite from Ōmuroyama, Izu, Japan (Kuno, 1965, table 5, nos. 8a and 8b). Although no melting history is available, it is not unreasonable, on petrographic and chemical grounds, to propose that this vein also should have a projected composition lying close to the boundary between the orthopyroxene+clinopyroxene and plagioclase+clinopyroxene fields.

It appears then that liquid compositions in the equilibrium orthopyroxene+plagioclase+clinopyroxene+liquid cannot be specifically defined when the quaternary analogy is used. Similar phase relations may occur in lavas with significantly differing bulk compositions, especially with respect to Fe and Si content.

According to Kuno (1965), and the results of extensive research at Pennsylvania State University (Roeder and Osborn, 1966), it is probable that  $K_{10}$  and  $K_{Fe}$  were produced by fractionation under conditions of low  $f_{O_2}$  while Jb evolved under contrasting conditions of high  $f_{O_2}$ , perhaps due to a higher magmatic  $H_2O$  content. It is interesting to compare the compositions of these three segregation veins with the range of residual liquid compositions in the system  $MgO-FeO-Fe_2O_3-CaAl_2Si_2O_8-SiO_2$  brought about by  $f_{O_2}$  variation (Roeder and Osborn, 1966, Fig. 14).

Another departure from the quaternary analogy, which is brought about by an increasing Fe/Mg ratio, has been demonstrated by Tilley *et al.* (1964, fig. 23). An increase in Fe/Mg ratio lowers the liquidus temperatures of natural basalts recorded in the quenching experiments. The effect of this on constructed phase diagrams is that thermal contouring can only be done for specified Fe/Mg ratios. In figs. 3 and 4, using the melting data of basalts with  $(FeO+Fe_2O_3)/(FeO+Fe_2O_3+MgO)$  ratios in the range 0.4–0.6, the temperature of the isobaric, pseudo-invariant equilibrium is c. 1135 °C and the temperature of the critical thermal maximum of the olivine+clinopyroxene+plagioclase+liquid equilibrium is of the order of 1160–80 °C.

<sup>1</sup> The orthopyroxene expected to nucleate from these evolved melts is presumably held in clinopyroxene solid solutions.

These temperatures compare with analogous temperatures in the synthetic system Fo-Di-Ab-Qz of 1120 and 1150 °C and in the synthetic system Fo-Di-An-Qz of 1250 and 1270 °C (Schaerer, 1967, figs. 8a and 8b).

By restricting the use of the  $R_2O_3$ -XO-YO-ZO<sub>2</sub> projection scheme to the illustration of the early crystallization features of tholeiitic magma, the resultant small departures from the quaternary analogy are tolerable. In the later stages of crystallization, as Fe/Mg and (Na+K)/Ca ratios build up, the effect of  $f_{O_2}$  becomes pronounced and additional phases such as ore and alkali feldspar may be precipitating; then the analogy has certainly broken down. Clearly the scheme is not suited to display the later stages of olivine tholeiite crystallization nor the crystallization behaviour of olivine-free basalts, andesites, and more evolved compositions.

Although 10 major and minor oxides are included in the pseudo-quaternary system, only 4 solid phases are considered. Variation in Na<sub>2</sub>O, K<sub>2</sub>O, TiO<sub>2</sub>, and Fe<sub>2</sub>O<sub>3</sub> contents must cause an apparent shift in the position of the phase boundaries constructed from basalt analyses and melting histories. As minor oxide variation in basic rocks is generally more pronounced between volcanic provinces than within one province, it may be that a natural phase diagram constructed from the data of one province will be inadequate to describe the crystallization behaviour of lavas in other provinces. An accurate assessment of shifts in the positions of boundary curves must, however, await a more thorough investigation of melting relations from tholeiitic provinces in addition to Hawaii. Nevertheless, because the oxide grouping rules (O'Hara, 1968, fig. 4) are standard, one can predict qualitatively the direction of shift as, say, K<sub>2</sub>O increases.

*Discussion.* As a check on the validity of the natural phase diagrams (figs. 3 and 4), the analyses of some porphyritic basalts of Kilauea and Mauna Loa have been projected in figs. 5 and 6. Since the melting relations of this group of lavas have not been determined, the phase boundaries in figs. 5 and 6 have been taken directly from figs. 3 and 4.

An examination of figs. 5 and 6 shows the phenocryst assemblages are consistent with the constructed phase boundaries. In particular, fig. 6 shows clearly an established, fundamental difference between Mauna Loa and Kilauea magma. In the former volcano orthopyroxene is an early crystallizing phase while in the latter volcano orthopyroxene is encountered only as a fourth silicate phase in the more evolved magmas.

A detailed examination of figs. 3 and 4 confirms a similar general consistency between the plotted position of the basalt analyses, the constructed phase boundaries, and the relevant melting relations. Not only the nature of the second and third phases to crystallize, but also the period of crystallization between the entry of the second and third solid phases are in most cases consistent with the relative positions of the composition points and the phase boundaries.

This consistency, it must be stressed, is in a general sense. Individual inconsistencies do exist; compare the melting relations of ML<sub>1887</sub> (oliv 1205 °C, opx 1175 °C, plag 1160 °C and cpx 1155 °C) with the crystallization history predicted in fig. 3 (olivine,



followed by orthopyroxene, then clinopyroxene, and finally plagioclase). This disagreement is probably greater than the degree of uncertainty in the determined melting relations but it does not destroy the over-all agreement between the phase relations in figs. 3–6 and the petrography, chemistry, and melting relations of the basalts.

Interpretation of the phase diagrams strongly supports the proposal that diversification of magma compositions during Hawaiian volcanic episodes is mainly due to crystal–liquid fractionation: consider, in figs. 3 and 4, the sequence of crystallization and the relative position of lava compositions to phase boundaries for the pair  $K_{1955/77}$  and  $K_{1955/82}$  and the series  $K_{1840pb}$ ,  $K_{1840b_1}$ , and  $K_{1840b_2}$ .

The importance of low-pressure crystal–liquid fractionation as a differentiation process in Hawaii has been widely recognized (Powers, 1955; Tilley, 1960 *a, b*). Nevertheless it is encouraging to find this feature is clearly demonstrated by the phase diagrams.

The author concludes that these partial phase diagrams (figs. 3–6) are a good representation of the phase relations that have controlled the surface and near-surface crystallization of Kilauea and Mauna Loa magmas.

Further examination of figs. 3–6 permits illustration of the following, more specific petrogenetic observations:

*Picrites* such as  $K_{1840pb}$ ,  $KI_{pb}$  and  $ML_{1868pb}$ , when projected from clinopyroxene, lie in relatively high-temperature areas of the olivine + clinopyroxene fields (figs. 4 and 6). When projected from olivine (figs. 3 and 5) these picrites plot along with the non-picritic lavas in a low-temperature part of the phase diagram. They lie close to the line representing the locus of liquid compositions in the equilibrium clinopyroxene + plagioclase + olivine + liquid. Furthermore, figs. 4 and 6 show that picrites such as  $ML_{1868pb}$  and  $KI_{pb}$  lie on olivine control lines joining the non-picritic lavas of the same eruption ( $ML_{1868b}$  and  $KI_g$ —the latter is actually the glass phase of such a lava) and the olivine composition point. This feature suggests that fractionation of olivine phenocrysts from a parental composition somewhere between, for example,  $ML_{1868pb}$  and  $ML_{1868b}$ , and on the olivine control line, has produced a residual liquid magma ( $K_{1868b}$ ) and an accumulative magma ( $K_{1868pb}$ ).

In the case of the lavas of the 1840 Kilauea Eastern Rift Zone eruption ( $K_{1840pb}$ ,  $K_{1840b_1}$ , and  $K_{1840b_2}$ ) fractionation of olivine phenocrysts alone cannot account for the variation. The fractionation of considerable amounts of clinopyroxene and plagioclase along with olivine is indicated by figs. 3 and 4—a feature previously noted by Tilley *et al.* (1963, table 4) on the basis of extract calculations. Using the analyses of the 1840 picrite basalt and basalt given by Macdonald (1949, table 6, nos. 1 and 2), Muir *et al.* (1957, p. 253) and Yoder and Tilley (1962, p. 388) have reached similar conclusions.

The series of submarine lavas from the Eastern Rift Zone of Kilauea ( $KE_{s-a-f}$ ) is of interest in this discussion of picrites. These compositions plot in the olivine primary phase volume and there is a correlation between distance from the isobaric, pseudo-invariant point in fig. 6, abundance of olivine phenocrysts, and apparent depth of eruption (Moore, 1965, fig. 3). These features suggest that either olivine

accumulation in near-cotectic Kilauean parental magma is more pronounced with depth, or that primary, or initial, Kilauean magma, with a composition well within the 1 atmosphere olivine primary phase volume, gradually changes its composition on ascent by a process of elutriation of olivine phenocrysts so that, on eruption, it has attained the near cotectic composition that is characteristic of Kilauean parental magma (Murata and Richter, 1966*b*, p. 198).

However, the plotted positions of this series of lavas in the olivine projection (fig. 5) show them to be near-cotectic with respect to the second and third solid phases. Moreover, in his petrographic descriptions, Moore (1965) notes small amounts of pyroxene (clinopyroxene?) and plagioclase phenocrysts in addition to abundant glass. These lavas must, therefore, have been erupted with compositions and at temperatures that suggest a genesis involving enrichment in cumulus olivine rather than a primitive picritic character.<sup>1</sup>

The examination of Hawaiian basalt analyses in this pseudo-quaternary system with natural phase boundaries is completely consistent with the conclusion, reached by many petrologists (e.g. Macdonald, 1949; Powers, 1955; Muir *et al.*, 1957), that the Hawaiian tholeiitic picrites are simply normal olivine tholeiites enriched in cumulus olivine.

*Parental Kilauean magma.* It is now relevant to investigate, with the aid of figs. 3–6, the question of the composition of the magma, or magmas, parental to the range of magmas produced by the low-pressure fractionation processes described above. The phase diagrams give no direct indication as to which magmas are parental in the crystal–liquid fractionation scheme. In fact, it is perfectly valid to interpret magmas with compositions such as  $K_{1840pb}$  and  $KI_{pb}$  as parental. However, such an interpretation is not in accordance with field evidence. According to the estimates of Powers (1955, p. 88) ‘olivine basalts’ make up 65–80 % of the Kilauean volcanic pile. Accumulative ‘picrite basalts’ and the more evolved ‘basalts’ account for only 5 % and 30–10 % respectively. As with all estimates of abundances, these must be treated with caution. They are, nevertheless, in good agreement with the density of composition points in figs. 3–6. Taking this field evidence into consideration, it is not unreasonable to consider the parental magma of Kilauea to be olivine tholeiite—a conclusion reached by Murata and Richter (1966*b*, p. 198).

The various glass, Pele’s Hair, and tachylyte compositions studied by Tilley *et al.* (1965) plot in the olivine primary phase volume of the pseudo-quaternary system (fig. 4). While some resorption of olivine phenocrysts by the liquid phase may have occurred in these specimens, it seems unlikely this could account for the observed consistent departures from the olivine+clinopyroxene+liquid equilibrium surface and the olivine+clinopyroxene+plagioclase+liquid equilibrium line.

Unless crystal–liquid fractionation was extremely selective, it is improbable that the

<sup>1</sup> The part of this argument based on the predicted near-simultaneous entry of the second and third solid phases would be invalid if there is a coincidence of the compositions of the 1 atmosphere, pseudo-invariant, tholeiitic liquid and the liquid produced by the partial melting of peridotite at depth, when both compositions are projected from olivine (O’Hara, 1965, p. 23; O’Hara, 1968, fig. 3; Davis and Schairer, 1965, p. 126).

picritic magmas, such as  $KI_{pb}$ , which lie on or near olivine control lines, could have developed from cotectic magmas. This implies that parental magmas must remain in the olivine+liquid condition for a period of time sufficient for the formation of magmas enriched in cumulus olivine and the complementary residual magmas.

Taken altogether, the above features suggest that the parental Kilauea magma, over the last 130 years at least, is an olivine tholeiite lying just below the liquidus in the olivine primary phase volume. Its temperature appears to be 10–20 °C above the temperature of attainment of the equilibrium olivine+clinopyroxene+liquid. Almost immediately after reaching this equilibrium plagioclase starts to crystallize as third solid phase. The most efficient crystal-liquid fractionation occurs whilst the magmas are in the olivine+liquid condition. At lower temperatures fractionation of clinopyroxene, plagioclase, and olivine is less effective; increased viscosity of the liquid and lower specific gravities of clinopyroxene and plagioclase may be significant factors. The best recent illustration of this cotectic fractionation is shown by the 1955 Eastern Rift lavas of which  $K_{1955/77}$  and  $K_{1955/82}$  are the two extreme compositions (Tilley, 1960a).

*Mauna Loa.* Although the melting data for Mauna Loa are less complete, the plotted positions of some prehistoric and historic lavas, together with the relevant petrographic descriptions, suggest that a situation analogous to that at Kilauea exists for this volcano. The important difference between Mauna Loa and Kilauea magma is that the former precipitates orthopyroxene at an earlier stage. The phase diagrams (figs. 4 and 6) indicate that orthopyroxene is the second crystalline phase. An examination of fig. 6 suggests that Mauna Loa parental magma reaches the summit reservoir in the olivine+liquid condition, but close to the isobaric, pseudo-invariant point.<sup>1</sup> This feature, and inspection of the phase diagrams (figs. 5 and 6), render unlikely the proposal that Mauna Loa magmas could be the residual magmas produced by crystal-liquid fractionation of Kilauea magma. Mauna Loa lavas contain too much modal, and in some instances normative, olivine to be residual magmas resulting from advanced fractionation. It is only the most evolved Kilauea magmas that contain small amounts of modal orthopyroxene, e.g.  $K_{1955/82}$  (Macdonald and Eaton, 1964, p. 85) and a specimen of the 1840 basalt from the same locality as  $K_{1840b_2}$  (Yoder and Tilley, 1962, p. 388). However, both  $K_{1955/82}$  and  $K_{1840b_2}$  contain significant normative quartz, 4.35 and 4.92 % respectively (Tilley, 1960a, table 5; Tilley *et al.*, 1963, table 3, no. 3), are olivine poor,<sup>2</sup> and represent a stage of differentiation characterized by removal of clinopyroxene and plagioclase accompanied by only minor olivine (Tilley *et al.*, 1963, p. 83; Tilley, 1960b, p. 496; Tilley and Scoon, 1961, p. 65). It is most improbable that evolved Kilauea magma of this type could be parental to the olivine-enriched picritic magmas e.g.  $ML_{1868pb}$ , which constitute a small, but significant, proportion of the visible Mauna Loa volcanic pile (Powers, 1955, p. 87).

This conclusion is supported by the lower average concentration levels of K, P,

<sup>1</sup> In all but the most basic Mauna Loa lavas quartz is present in the norm. Under equilibrium conditions the olivine present in these Mauna Loa lavas would be totally resorbed.

<sup>2</sup> The olivine in  $K_{1955/82}$  is considered to have been undergoing resorption at the time of eruption (Macdonald and Eaton, 1964, p. 86).

and certain trace elements in Mauna Loa basalts (table 1). During near-surface fractionation of tholeiitic magma these elements are concentrated in residual liquids.

Mauna Loa magma must, therefore, have a genesis that is independent of Kilauea magma under near-surface conditions. This aspect of Hawaiian volcanism has been stressed by Tilley and Scoon (1961).

*Conclusions.* It is concluded that the  $R_2O_3$ — $XO$ — $YO$ — $ZO_2$  data projection scheme allows one to reconstruct diagrammatically the probable phase relations that control the near-surface crystallization of Kilauea and Mauna Loa basaltic magma. Use of the projection scheme offers an additional method of presenting and interpreting the variation in lava compositions.

The petrogenetic conclusions reached are, in general, compatible with those already established on the basis of petrographic observations and extract calculations. Nevertheless, the use of natural phase diagrams of the type described above is recommended whenever the petrographic descriptions or melting relations are sufficiently well known to allow construction of phase boundaries.

Use of such natural phase diagrams facilitates the comparison between crystallization behaviour in synthetic systems and in the complex natural systems, and encourages one to consider the crystallization of magmas from a phase equilibrium standpoint. When the calculations are computerized the projection scheme is easy to use and interpret.

*Acknowledgements.* The author wishes to acknowledge the encouragement and advice freely given by Dr. M. J. O'Hara during the preparation of this paper. Thanks are also due to Drs. M. G. Best and K. G. Cox for reviewing a draft of the manuscript.

#### REFERENCES

- BOWEN (N. L.), 1914. *Amer. Journ. Sci.* **38**, 207.  
 — 1928. *The Evolution of the Igneous Rocks*. Princeton (Princeton University Press) [M.A. 4-123].  
 COHEN (L. H.), ITO (K.), and KENNEDY (G. C.), 1967. *Amer. Journ. Sci.* **265**, 475.  
 COOMBS (D. S.), 1963. *Mineralogical Society of America Special Paper* **1**, 227 [M.A. 17-323].  
 DAVIS (B. T. C.) and SCHAIRER (J. F.), 1965. *Carnegie Inst. Washington Year Book*, **64**, 123.  
 FUDALI (R. F.), 1965. *Geochimica Acta*, **29**, 1063 [M.A. 17-475].  
 HAMILTON (D. L.), BURNHAM (C. W.), and OSBORN (E. F.), 1964. *Journ. Petrology*, **5**, 21 [M.A. 16-625].  
 KUNO (H.), 1965. *Ibid.* **6**, 302 [M.A. 17-625].  
 — YAMASAKI (K.), IIDA (C.), and NAGASHIMA (K.), 1957. *Japan. Journ. Geol. Geog.* **28**, 179 [M.A. 14-214].  
 MCBIRNEY (A. R.) and WILLIAMS (H.), 1965. *University of California, Berkeley, Publications in Geological Sciences*, **55** [M.A. 17-553].  
 MACDONALD (G. A.), 1949. *Bull. Geol. Soc. Amer.* **60**, 1541 [M.A. 11-151].  
 — and EATON (J. P.), 1964. *U.S. Geol. Surv. Bull.* **1171**.  
 — and KATSURA (T.), 1964. *Journ. Petrology*, **5**, 82 [M.A. 16-656].  
 MOORE (J. G.), 1965. *Amer. Journ. Sci.* **263**, 53.  
 MUIR (I. D.) and TILLEY (C. E.), 1963. *Ibid.* **261**, 111.  
 — — 1964. *Geol. Journ.* **4**, 143 [M.A. 17-324].  
 — — and SCOON (J. H.), 1957. *Amer. Journ. Sci.* **255**, 241 [M.A. 14-146].  
 MURATA (K. J.) and RICHTER (D. H.), 1966a. *U.S. Geol. Surv. Prof. Paper* **537-A**.  
 — — 1966b. *Amer. Journ. Sci.* **264**, 194 [M.A. 18-59].  
 NICHOLLS (G. D.), NALWALK (A. J.), and HAYS (E. E.), 1964. *Marine Geology*, **1**, 333.  
 O'HARA (M. J.), 1965. *Scot. Journ. Geol.* **1**, 19 [M.A. 17-324].  
 — 1968. *Earth-Science Reviews*, **4**, 69.

- OSBORN (E. F.) and TAIT (O. B.), 1952. *Amer. Journ. Sci.*, Bowen volume, 413 [M.A. 12-81].
- POWERS (H. A.), 1955. *Geochimica Acta*, 7, 77.
- PRINZ (M.), 1967. In HESS (H. H.) and POLDERVAART (A.) (eds.) *Basalts: The Poldervaart Treatise on Rocks of Basaltic Composition*, 1, 271. New York (Interscience).
- RICHTER (D. H.), AULT (W. U.), EATON (J. P.), and MOORE (J. G.), 1964. *U.S. Geol. Surv. Prof. Paper* 474-D.
- ROEDER (P.L.) and OSBORN (E. F.), 1966. *Amer. Journ. Sci.* 264, 428 [M.A. 18-172].
- SCHAIRER (J. F.), 1967. In ABELSON (P. H.) (ed.) *Researches in Geochemistry*, 2, 568. New York (Wiley).
- TILLEY (C. E.), 1960a. *Journ. Petrology*, 1, 47 [M.A. 14-436].
- 1960b. *Geol. Mag.* 97, 494 [M.A. 15-227].
- and SCOON (J. H.), 1961. *Amer. Journ. Sci.* 259, 60 [M. A. 15-227].
- YODER (H. S., Jnr.), and SCHAIRER (J. F.), 1963. *Carnegie Inst. Washington Year Book*, 62, 77.
- — — 1964. *Ibid.* 63, 92.
- — — 1965. *Ibid.* 64, 69.
- — — 1966. *Ibid.* 65, 260.
- WENTWORTH (C. K.) and WINCHELL (M.), 1947. *Bull. Geol. Soc. Amer.* 58, 49.
- WILCOX (R. E.), 1954. *U.S. Geol. Surv. Bull.* 965-C.
- YODER (H. S., Jnr.) and TILLEY (C. E.), 1962. *Journ. Petrology*, 3, 342 [M.A. 16-475].

## APPENDIX

*Melted basalts*

- E<sub>1</sub>: Olivine basalt, Eldgja-Katla lava, Iceland (Tilley *et al.*, 1964, table 1). Plag 1140°, cpx 1140°, oliv 1120°. Ref. 2.
- E<sub>2</sub>: Olivine basalt, Eldgja-Katla lava, Iceland (Tilley *et al.*, 1964, table 1). Plag 1120°, cpx 1110°, oliv 1110°. Ref. 2.
- Hu: Prehistoric alkali basalt, Hualalai, Hawaii (Yoder and Tilley, 1962, table 2, no. 20). Oliv 1235°, plag 1160°, cpx 1155°. Yoder and Tilley, 1962, fig. 6.
- Ka: Hypersthene-olivine basalt, Kauai, Hawaiian Islands (Tilley *et al.*, 1963, table 3, no. 4). Oliv 1385°, opx 1170°, plag 1155°, cpx 1140°. Ref. 1.
- Ko: Hypersthene mela-basalt, Koolau series, Oahu, Hawaiian Islands (Wentworth and Winchell, 1947, table 4, no. 4). Oliv 1245°, opx 1165°, plag 1165°, cpx 1135°. Ref. 1.
- K<sub>Fe</sub>: Iron-rich segregation in Kilauea tholeiite, Hawaii (Kuno *et al.*, 1957, table 5, no. 6). Plag 1080°, cpx 1080°. Ref. 1.
- K<sub>10</sub>: Iron-rich segregation in basalt, Ō-shima Island, Japan (Tilley *et al.*, 1963, table 3, no. 7). Cpx 1120°, plag 1110°. Ref. 1.
- K<sub>p</sub>: Prehistoric flow of Kilauea, Hawaii (Yoder and Tilley, 1962, table 2, no. 7). Oliv 1195°, cpx 1170°, plag 1160°. Ref. 1.
- K<sub>1840b1</sub>: 1840 olivine-bearing lava of upper vents, Kilauea, Hawaii (Tilley *et al.*, 1963, table 3, no. 2). Oliv 1205°, plag 1135°, cpx 1135°. Ref. 1.
- K<sub>1840b2</sub>: 1840 lava of upper vents, Kilauea, Hawaii (Tilley *et al.*, 1963, table 3, no. 3). Plag 1150°, cpx 1145°. Ref. 1.
- K<sub>1840pb</sub>: 1840 picrite basalt, lava of lower vents, Kilauea, Hawaii (Tilley *et al.*, 1963, table 3, no. 1). Oliv 1435°, plag 1165°, cpx 1165°. Ref. 1.
- K<sub>1920ph</sub>: Pele's Hair, 1920 eruption of Kilauea, Hawaii (Tilley *et al.*, 1965, table 1). Oliv 1170°, cpx 1160°, plag 1155°. Ref. 3.
- K<sub>1921</sub>: 1921 lava of Kilauea, Hawaii (Yoder and Tilley, 1962, table 2, no. 7). Oliv 1235°, plag 1170°, cpx 1170°. Ref. 1.

- K<sub>1921</sub>** : 1921 lava of Kilauea, Hawaii (Fudali, 1965, table 1, no. 1). Oliv 1210°, cpx 1165°, plag 1165°. Ref. 3.
- K<sub>1921ph</sub>**: Pele's Hair, 1921 eruption of Kilauea, Hawaii (Tilley, 1960a, table 1, no. 4). Oliv 1180°, cpx 1160°, plag 1155°. Ref. 3.
- K<sub>1921</sub>** : Tachylyte, 1921 eruption of Kilauea, Hawaii (Tilley, 1960a, table 1, no. 6). Oliv 1175°, cpx 1165°, plag 1155°. Ref. 3.
- K<sub>1955/77</sub>**: 1955 lava of Kilauea, Hawaii (Tilley, 1960a, table 4, no. 77). Oliv 1155°, plag 1155°, cpx 1155°. Ref. 1.
- K<sub>1955/82</sub>**: Most evolved lava of 1955 eruption, Kilauea, Hawaii (Tilley, 1960a, table 4, no. 82). Plag 1135°, oliv 1125°, cpx 1125°. Ref. 1.
- K<sub>1960b</sub>**: 1960 (13th Jan.) lava of Kilauea, Hawaii (Yoder and Tilley, 1962, table 2, no. 7a). Plag 1160°, cpx 1160°. Ref. 1.
- K<sub>1963a1</sub>**: Lava of 1963, Alae Lake, Kilauea, Hawaii (Tilley *et al.*, 1966, table 5, no. 5). Cpx 1190°, oliv 1180°, plag 1155°. Ref. 4.
- KI<sub>g</sub>**: Glass from 1959 picrite basalt (KIpb) Kilauea Iki, Hawaii (Murata and Richter, 1966a, table 4, no. S-5g). Oliv. 1225°, cpx 1165°, plag 1155°. Ref. 3.
- KI<sub>pb</sub>**: 1959 (18 Nov.) picrite basalt, Kilauea Iki, Hawaii (Murata and Richter, 1966a, table 1, no. S-5). Oliv 1425°, cpx 1165°, plag 1150°. Ref. 3.
- MK**: Picrite basalt of ankaramitic character, Mauna Kea, Hawaii (Tilley *et al.*, 1964, table 1). Oliv 1420°, cpx 1210°, plag 1165°. Ref. 2.
- ML<sub>1887</sub>**: 1887 lava of Mauna Loa, Hawaii (Yoder and Tilley, 1962, table 2, no. 5). Oliv 1205°, opx 1175°, plag. 1160°, cpx 1155°. Ref. 1.
- ML<sub>1935</sub>**: 1935 pahoehoe flow of Mauna Loa, Hawaii (Tilley *et al.*, 1964, table 1). Oliv 1180°, cpx 1180°, plag 1160°. Ref. 2.
- N**: Tachylyte margin of basalt, mid-Atlantic ridge (Nicholls *et al.*, 1964, table 1, no. 2). Oliv 1245°, plag 1215°, cpx 1165°. Ref. 3.
- NM<sub>5</sub>**: Glass prepared from olivine tholeiite, San Juan Mts., New Mexico (Yoder and Tilley, 1962, table 11, no. 3). Plag 1195°, oliv 1185°, cpx 1185°. Ref. 1.
- Nic<sub>324</sub>**: Tholeiite, Masaya Caldera, Nicaragua (McBirney and Williams, 1965, table 5, no. 16). Plag 1165°, cpx 1155°, oliv 1145°. Ref. 4.
- PG**: Columbia River basalt, Picture Gorge, Oregon (Hamilton *et al.*, 1964, table 1, no. 1). Plag. 1155°, cpx 1155°. Ref. 2.
- P<sub>a</sub>**: Hypersthene andesite of 1 September 1950, Paricutin, Mexico (Wilcox, 1954, table 2, no. 19). Plag 1197°, opx 1145°. Ref. 4.
- P<sub>hab</sub>**: High-alumina basalt of March 1944, Paricutin, Mexico (Tilley *et al.*, 1966, table 5, no. 3). Plag. 1220°, oliv 1215°, cpx 1155°. Ref. 4.
- W**: High-alumina basalt, Medicine Lake Highlands, California (Yoder and Tilley, 1962, table 2, no. 16). Oliv 1240°, plag 1240°, cpx 1165°. Ref. 1.

Temperatures, in °C, are those at which the phases indicated disappear; oliv being olivine; plag, plagioclase; cpx, clinopyroxene; and opx, orthopyroxene. Melting histories are taken from the following sources:

Ref. 1—Tilley *et al.* (1963)

Ref. 2—Tilley *et al.* (1964)

Ref. 3—Tilley *et al.* (1965)

Ref. 4—Tilley *et al.* (1966)

*Other basalts*

- $J_a$ : Olivine andesite of Ōmuro-yama Volcano, Izu, Japan. Sparse phenocrysts of olivine and plagioclase, the olivine being rimmed by orthopyroxene (Kuno, 1965, table 5, no. 8A).
- $J_b$ : Segregation vein in  $J_a$  consisting of plagioclase, clinopyroxene, orthopyroxene, and ore in a brown glass (Kuno, 1965, table 5, no. 8B).
- $K_{1868-a}$ : 1868 flow of Kilauea, Hawaii. Contains conspicuous olivine, clinopyroxene, and plagioclase phenocrysts (Tilley and Scoon, 1961, table 1, no. 1).
- $K_{1868-b}$ : 1868 flow of Kilauea, Hawaii. Carries olivine, clinopyroxene, and plagioclase phenocrysts (Tilley and Scoon, 1961, table 1, no. 2).
- $K_{1868-c}$ : 1868 flow of Kilauea, Hawaii. Tachylyte from spatter cone with a few olivine phenocrysts and smaller crystals of plagioclase and clinopyroxene (Tilley and Scoon, 1961, table 1, no. 3).
- $K_{1959-a}$ : 1959 lava of Kilauea, Hawaii. Has conspicuous olivine phenocrysts; picritic character (Tilley, 1960b, table 1, no. 2).
- $K_{1959-b}$ : 1959 lava of Kilauea, Hawaii. Carries conspicuous phenocrysts of olivine in a glassy base (Tilley, 1960b, table 1, no. 1).
- $K_{1960-a}$ : Olivine tholeiite, 1960 flank eruption of Kilauea, Hawaii: lava of 18 February. Contains abundant olivine phenocrysts (Muir and Tilley, 1963, table 8, no. 4).
- $KE_{1961-a}$ : Lava of 1961 summit eruption, Kilauea, Hawaii. Contains rare olivine phenocrysts (Richter *et al.*, 1964, table 4, no. 4).
- $KE_{1961-b}$ : Lava of 1961 flank eruption, Kilauea, Hawaii. Contains very rare microphenocrysts of olivine and clinopyroxene (Richter *et al.*, 1964, table 4, no. 5).
- $KE_{1961-c}$ : Lava of 1961 flank eruption, Kilauea, Hawaii. Contains 5 % olivine phenocrysts and microphenocrysts of clinopyroxene and plagioclase (Richter *et al.*, 1964, table 4, no. 7).
- $KE_{1961-d}$ : Lava of 1961 flank eruption, Kilauea, Hawaii. Carries 7 % olivine phenocrysts with rare microphenocrysts of clinopyroxene and plagioclase (Richter *et al.*, 1964, table 4, no. 8).
- $KE_{s-a}$ : Submarine basalt from Eastern rift zone, Hawaii. 94 % glass, 1.9 % oliv, 3.1 % pyroxene, and 1.0 % plag (Moore, 1965, table 2, no. 1).
- $KE_{s-b}$ : Submarine basalt from Eastern rift zone, Hawaii. 89.4 % glass, 8.7 % oliv, 1.1 % pyroxene, and 1.1 % plag (Moore, 1965, table 2, no. 2).
- $KE_{s-c}$ : Submarine basalt from Eastern rift zone, Hawaii. 86.4 % glass, 13.5 % oliv, and 0.1 % pyroxene (Moore, 1965, table 2, no. 3).
- $KE_{s-d}$ : Submarine basalt from Eastern rift zone, Hawaii. 66.3 % glass, 21.9 % oliv, 5.5 % pyroxene, and 6.3 % plag (Moore, 1965, table 2, no. 5).
- $KE_{s-e}$ : Submarine basalt from Eastern rift zone, Hawaii. 81.4 % glass, 14.4 % oliv, 2.5 % pyroxene, and 1.7 % plag (Moore, 1965, table 2, no. 7).
- $KE_{s-f}$ : Submarine basalt from Eastern rift zone, Hawaii. 69.7 % glass, 23.2 % oliv, 5.6 % pyroxene, and 1.5 % plag (Moore, 1965, table 2, no. 9).
- $ML_{p-a}$ : Pahoehoe phase of prehistoric lava, Mauna Loa, Hawaii. Carries phenocrysts of olivine, hypersthene, clinopyroxene, and plagioclase (Tilley and Scoon, 1961, table 3, no. 1).

- ML<sub>p-b</sub>: Aa phase of prehistoric lava, Mauna Loa, Hawaii. Carries phenocrysts of olivine, hypersthene clinopyroxene, and plagioclase (Tilley and Scoon, 1961, table 3, no. 2).
- ML<sub>p-c</sub>: Prehistoric lava, Mauna Loa, Hawaii. Carries phenocrysts of olivine, hypersthene, clinopyroxene, and plagioclase (Tilley and Scoon, 1961, table 3, no. 3).
- ML<sub>1868pb</sub>: Picrite basalt, lava of 1868, Mauna Loa, Hawaii. Conspicuous olivine phenocrysts in addition to phenocrysts of clinopyroxene, hypersthene, and plagioclase (Tilley and Scoon, 1961, table 2, no. 1).
- ML<sub>1868p</sub>: Basalt lava of 1868, Mauna Loa, Hawaii. Carries same phenocryst assemblage as the picritic basalt (ML<sub>1868pb</sub>) but is poorer in olivine phenocryst content (Tilley and Scoon, 1961, table 2, no. 2).
- ML<sub>1881</sub>: Lava of 1881, Mauna Loa, Hawaii. (Analysis given by Tilley and Scoon, 1961, table 3, no. 5.)
- ML<sub>1926-a</sub>: Basalt, 1926 eruption of Mauna Loa, Hawaii (Macdonald, 1949, table 6, no. 6).
- ML<sub>1926-b</sub>: Basalt, pumiceous phase, 1926 eruption, Mauna Loa, Hawaii (Macdonald, 1949, table 6, no. 7).
- ML<sub>1942-a</sub>: Basalt, latest lava of the 9200-ft vent, Mauna Loa, Hawaii (Macdonald, 1949, table 6, no. 4).
- ML<sub>1942-b</sub>: Basalt, earliest lava of the 9200-ft vent, Mauna Loa, Hawaii (Macdonald, 1949, table 6, no. 5).

[Manuscript received 30 October 1968]